L-band Aperture Synthesis Radiometry: Hardware Requirements and System Performance*

I. Corbella, F. Torres, A. Camps, J. Bará, N. Duffo. M. Vall-llossera
Department of Signal Theory and Communications. Universitat Politècnica de Catalunya. UPC Campus Nord. C/ Jordi Girona 1,3. 08034 Barcelona (Spain)
Telephone: +34 93 401 72 28. Fax: +34 93 401 72 32. E-mail (corbella@tsc.upc.es)

INTRODUCTION

Aperture synthesis radiometry is becoming a feasible concept for imaging applications, especially at low microwave frequencies where it takes clear advantage of the absence of mechanical antenna motion. A 2D interferometric radiometer consists of a large number of receivers with small antennas distributed along a 2D structure, and the brightness temperature image is formed by inversion of the measured cross-correlation between all pairs of antennas. This is the concept of MIRAS (MIcrowave Radiometer by Aperture Synthesis), the core instrument of the SMOS (Soil Moisture and Ocean Salinity) mission selected by the European Space Agency (ESA) and planned to be launched in 2005. In its preliminary design, MIRAS receivers are uniformly distributed along a Y-shape structure and work at L-Band.

This approach, however, poses a challenge in the specifications required for the receivers: a) The short integration time due to the platform motion strongly limits the achievable sensitivity, b) the spatial resolution is determined by the structure dimensions -which cannot be made arbitrarily large- and c) the radiometric accuracy depends on the non ideal behavior of the receivers, although, to some extent can be corrected by internal calibration.

This paper contributes to define the main trade-off between hardware requirements and system performance of this complex instrument.

RECEIVER FREQUENCY PLAN

A typical MIRAS receiver (Fig. 1) includes an RF section -with an input switch, a filter and an amplifier-, a phase/quadrature frequency down-converter, two two-level (sign function) quantizers and samplers. The RF bandwidth is limited to the reserved band 1400-1427 MHz, but to avoid interference from L-band radars and other services at adjacent frequencies, the input RF filter band is fixed at 1404-1423 MHz. The in-phase (i) and quadrature (q) outputs of all receivers are sent to a matrix of 1 bit digital correlators located in the hub. Complex correlation is achieved from two real correlations: i⊗i gives the real part and q⊗i the imaginary part. The use of one-bit two level digital correlators allows high level of integration, lower data rate and moderate power consumption. On the other hand, the radiometric sensitivity is degraded by a factor depending on the sampling rate and the intermediate frequency (IF) band.

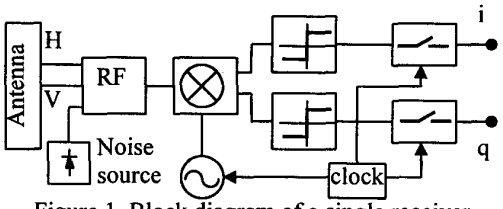

Figure 1. Block diagram of a single receiver

Clock frequency and IF band

The IF band is set by the local oscillator (LO) frequency. To avoid reducing the signal bandwidth (and thus the sensitivity) the receiver operates in (upper) single side band mode, which means that the LO frequency is set outside the RF band, and the image band is filtered. The IF band goes then from 1404-f_{LO} to 1423-f_{LO} MHz. The system clock is used both to drive the samplers and to lock the LO frequency, so this one is a multiple of the system clock. To agree with the Nyquist sampling criterion the clock frequency must be twice the largest frequency in the band. However, a high clock frequency increases the data rate and creates technological design problems in the correlator. So, the lowest possible IF frequency is desired but, on the other hand, low IF means closer image band, and the image rejection becomes worse. Furthermore, since the filter is not of ideal rectangular shape, there is always a given amount of aliasing, which in any case has to be evaluated. All this ultimately affects the error in the measured correlation for a given integration time, which can be quantified by the use of the so-called "*effective integration time*" in all radiometric sensitivity computations.

Effective integration time

The output of a real digital correlator is a random signal:

$$r = \frac{1}{N}\sum_{i=1}^{N}\rho_i , \qquad (1)$$

where N is the total number of samples and $\rho_i = g[b_1(t_i)]\cdot g[b_2(t_i)]$, being g[] the non-linear quantizing function and b_1 and b_2 the correlator input signals (Gaussian). The sampling times are $t_i = t_0+(i-1)/f_s$ being t_0 an arbitrary time origin and f_s the sampling (clock) frequency. The variance of r is given by ([1] chapter 7):

$$\sigma_r^2 = \frac{\sigma_\rho^2}{N} + \frac{2}{N^2}\sum_{i=1}^{N-1}(N-i)\cdot\left(R_\rho(iT_s)-\bar{\rho}^2\right), \qquad (2)$$

* Work supported under contract by CASA Space Division (Spain) and the European Space Agency (ESA)

where R_ρ is the autocorrelation function of ρ, σ_ρ^2 its variance and $\bar{\rho}$ its mean, which turns out to be equal to that of r. For *uncorrelated* samples this equation is reduced to the known result $\sigma_r^2 = \sigma_\rho^2/N$, which allows to define, in the general case of correlated samples, the effective number of samples as $N_{eff} = \sigma_\rho^2/\sigma_r^2$

If the integration time is limited to τ, the total number of samples is $N \approx f_s\tau$. At the Nyquist sampling rate $f_s=2B$ where B the signal bandwidth, so $N_{Nyquist}=2B\tau$. Since in this case the samples are uncorrelated, the effective integration time can be defined as:

$$\tau_{eff} \overset{\Delta}{=} \frac{N_{eff}}{2B} = \frac{\sigma_\rho^2/\sigma_r^2}{2B} \tag{3}$$

Now, introducing this definition in (2), and using the approximations suggested in [2] for one bit two level correlators, the effective integration time can easily be computed as a function of the frequency clock, taking into account different filter shapes and LO frequencies.

Figure 2 shows the effective integration time for three LO frequencies as a function of clock frequency. The autocorrelation function $R_\rho(t)$ in (2) has been computed by inverse Fourier Transform from the measured frequency responses of two actual filters manufactured by Matra Marconi Space (UK) especially for the MIRAS project.

This figure shows that oversampling increases the effective integration time if quantization is used. Moreover shifting the band to higher frequencies (higher LO) decreases the effective integration time, unless the clock frequency is increased at least to twice the maximum frequency of the band, regardless of the signal bandwidth[1]. The known result $\tau_{eff}=\tau/2.46$ given in [2] and experimentally verified in [3] corresponds here to a LO frequency of 1404 MHz and clock frequency of 38 MHz. The small discrepancy is due to the use of a real filter instead of an ideal rectangular one.

Since the LO frequency must be a multiple of the clock frequency, a good choice is f_{LO}=1396 MHz and f_{clk}=55.84 MHz, which corresponds to an IF band of 8 to 27 MHz. With these values, the effective integration time becomes $\tau_{eff}=0.55\ \tau$, which once substituted in the equation for radiometric sensitivity [4], gives $\Delta T \approx 5K$ for a 200K constant scene.

RADIOMETRIC ACCURACY

A 2D interferometric radiometer is based on the integral relation existing between the brightness temperature map of an extended source and the cross-correlation between pairs of antennas (visibility function). In normalized version, it is:

$$\mu(u,v) = \Im\left[\overline{T}(\xi,\eta)\right] \tag{4}$$

[1] The case of band pass sampling is not covered here.

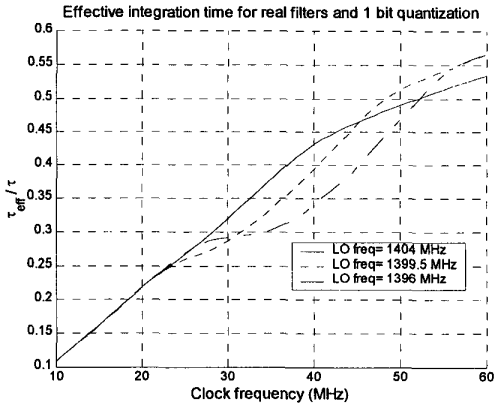

Figure 2 Effective integration time

where the symbol $\Im$ stands for a 2D integral operator, which is reduced to a Fourier Transform when decorrelation effects are negligible and the antennas are identical. In this transformation (ξ,η) are the directing cosines and (u,v) the projections over the XY axes of the antenna spacing, normalized to the nominal center frequency. The function to which the operator is applied is the so-called *normalized modified* temperature, defined as:

$$\overline{T} = \frac{1}{T_A}\frac{T_B(\xi,\eta)}{\sqrt{1-\xi^2-\eta^2}}\frac{F_{nk}(\xi,\eta)F_{nj}^*(\xi,\eta)}{\sqrt{\Omega_k\Omega_j}}, \tag{5}$$

being T_B the brightness temperature map, T_A the antenna temperature, $F_{nk,j}$ the normalized voltage pattern of antennas k and j forming a baseline, and $\Omega_{k,j}$ their equivalent solid angle. In the above expression, the antenna temperature is considered the same for all antennas and very accurately measured using a dedicated total power radiometer located in the center of the array.

Due to system imperfections, the retrieved modified temperature of a given pixel differs from the actual one, thus producing a distorted image. The *radiometric accuracy* is defined [5] as the root-mean square of the temperature errors of the individual pixels, namely:

$$\Delta T = \sqrt{\frac{1}{M-1}\sum_{i=1}^{M}\left[\hat{T}-T\right]^2} \tag{6}$$

being T the (non-normalized) modified temperature $T = \overline{T}T_A$ and $\hat{T}$ its estimation using the actual instrument. The above formula is applied to M pixels, corresponding only to the central part of the field of view to avoid aliasing effects. The test scene consists of a constant temperature of 200K over the Earth and 0K in the sky.

Sensitivity of errors to radiometric accuracy

All imperfections in the receivers or antennas contribute to the degradation of the radiometric accuracy, some of them having greater impact than others. Equation (6) is useful to compute the contribution of a given error to ΔT. Numerical computation of ΔT for Gaussian random errors in the

receivers or antennas shows that this is linearly dependent of the standard deviation of the error, which allows to define the *sensitivity* of the error to radiometric accuracy S_j as:

$$\Delta T\big|_j \approx S_j \sigma_{error\,j} . \quad (7)$$

The maximum allowable error in a given parameter can be easily computed from (7), provided the maximum impact that produces in the radiometric accuracy is established. If all contributions are considered independent from each other, the *total radiometric accuracy* turns out to be the quadratic summation of all of them, namely:

$$\Delta T_{total} = \sqrt{\sum_{j=1}^{n} \left[\Delta T\big|_j\right]^2} , \quad (8)$$

being n the number of individual contributions to ΔT.

Accuracy improvement by calibration

Periodic calibration is needed so as to estimate the different errors in order to correct them in the inversion procedure. Radiometric accuracy is then determined by the residual errors after correction. In any case, the specifications of the instrument must be established so as to have the total radiometric accuracy, after calibration, below a given specified value, which is eventually set by the scientific requirements of the mission. As shown in Fig 1, internal calibration is performed by periodically injecting noise to the receivers. Two sources of noise are used: uncorrelated (for the offset) and correlated. Due to the large dimensions of the array, correlated noise cannot be accurately distributed to all receivers, but only to those of the hub. For the rest, a distributed approach using several sources must be used [6]. This reduces the effectiveness of the calibration mechanism, getting as a result some residual non-separable amplitude and phase errors, having high impact on accuracy.

Antenna errors cannot be corrected using noise injection so, to achieve low impact on accuracy, good on-ground characterization is needed. This must be performed with the antennas mounted and loaded in the same conditions as in normal instrument operation, so as to include mutual coupling effects. Low drift in the lifetime must be assumed.

Accuracy budged

Table 1 shows the computed sensitivities of the main error sources along with their contribution to radiometric accuracy given reasonable values. In this table the antenna pattern errors must be understood as accuracy in the on-ground measurement. The separable phase error includes phase differences in antenna path (before injection) and in the noise distribution network. Separable amplitude errors are estimated from the accuracy of measuring the noise temperature of the receivers, and non-separable amplitude and phase errors assume that complete correlated noise is only injected in the hub antennas, using a distributed approach for the rest [6]. The *other* sources in the last line of Table 1 refer mainly to cross-polarization and correlators offset, not included in the previous lines.

Table 1. Contribution of errors to accuracy

Error	Sensitivity	σ_{error}	ΔT (K)
Antenna pattern			
phase ripple	1.48 K/°	0.5°	0.74
amplitude ripple	1.06 K/%	0.5%	0.53
Antenna phase center			
x-y uncertainty	2.65 K/mm	0.25mm	0.66
z axis uncertainty	0.53 K/mm	1 mm	0.53
Receiver errors			
Separable amplitude	0.59 K/%	0.68%	0.4
Separable phase	0.36 K/°	0.9°	0.32
Quadrature	0.36 K/°	0.1°	0.04
Non-separable amplitude	0.28 K/%	1.5%	0.44
Non-separable phase	0.5 K/°	0.8°	0.4
Other			1.0
TOTAL ACCURACY			**1.8**

CONCLUSION

The main hardware requirements for MIRAS, a 1.4 GHz aperture synthesis radiometer currently being developed for the ESA mission SMOS, have been studied in terms of their impact on system performance. First, the clock frequency and IF band and their contribution to the effective integration time. Then various receiver and antenna errors affecting the radiometric accuracy. At the end, the total accuracy expected for such instrument is estimated.

REFERENCES

[1] F. T. Ulaby, R.K. Moore, A.K. Fung "Microwave Remote Sensing, active and passive" volume II. Addison-Wesley 1981.

[2] J.B. Hagen, D.T. Farley, "Digital correlation techniques in radio science". Radio science, vol 8 numbers 8,9, pp 775-784, August-September 1973.

[3] Camps, A., J. Bará, F. Torres, I. Corbella, F. Monzón, "Experimental Validation of radiometric sensitivity in correlation radiometers", Electronics Letters, December 1998, Vol. 34, No 25, p. 2377

[4] Camps, A., I. Corbella, J. Bará, F. Torres, "Radiometric Sensitivity Computation in Aperture Synthesis Interferometric Radiometry", IEEE Trans. on Geoscience and Remote Sensing, March 1998, vol 36, No 2, pp 680-685.

[5] Torres, F., A. Camps, J. Bará, I. Corbella, "Impact of Receiver Errors on the Radiometric Resolution of Large 2D Aperture Synthesis Radiometers. Study Applied to MIRAS", Radio Science, March-April 1997, Vol 32, N° 2., pp 629-642.

[6] Corbella, I., F. Torres, A. Camps, J. Bará, "A new calibration technique for interferometric radiometers", European Symposium on Aerospace Remote Sensing, Conference on Sensors, Systems and Next Generation Satellites IV, September, 1998, Barcelona, SPAIN.